Confined air-liquid drainage : local analysis and invasion percolation model

F. Plouraboué[1], S. Geoffroy[1,2], F. Flukiger[1], O.Amyot[1], M. Prat[1]
[1] *Institut de Mécanique des Fluides de Toulouse, UMR 5502 CNRS, (France)*
[2] *Laboratoire Génie Mécanique, INSA, 135 av Rangeuil, 31077 Toulouse (France)*

This paper studies drainage of a wetting liquid by non wetting air between two confined rough solid surfaces. From convergence of asymptotic, numerical and experimental analyses, we found simple expressions for the air finger width and total curvature invading a single saddle-point as a function of its aspect ratio. The result of this local analysis is applied to a new invasion percolation numerical model which is compared to experiments involving drainage between complicated rough surfaces.

I. INTRODUCTION

Studying flows between two confined solid surfaces is interesting in different contexts such as fracture flows, microfluidic[1] or water-tightness[2]. We chose to focus on drainage of a wetting liquid by non wetting air in the limit of small Reynolds and capillary numbers. In this limit pressure driven air invasion through the wetting liquid is dominated by capillary forces. Moreover the viscous pressure drop is negligible and the pressure inside the liquid and the air is uniform. In this case the invasion process is controlled by the liquid-gas interface curvature, in keeping with Laplace law. The invasion of air in complicated geometries, is controlled by bottom-neck constrictions that the uniform pressure inside the air finger has to overcome. In section II we begin by examining the air invasion at the local level. From the obtained results section III proposes a new percolation invasion model which is compared with experiments.

II. LOCAL ANALYSIS FOR A SINGLE CHANNEL

This section first analyses the drainage in a longitudinally invariant channel in the x direction — see fig 1a, with associated depth $h(y)$. This analysis will then be complemented by a comparison with a longitudinally constricted channel, with small longitudinal variations along the x direction.

• Experimental description : Mini-channels with $h_0 = 1mm$ have been built with an automatic micro-machining device which has carved a polymeric material, given a specified depth function $h(y)$ with 20 micron precision in every (x, y, z) direction. Experiments were carried out by slowly pumping out a perfectly wetting silicon oil, with associated capillary number smaller than 10^{-3}. The finger width f^∞/ℓ display a very small influence of the capillary number in the range 10^{-3} to 10^{-5}. f^∞ is controlled by the finger tip curvature, because the surface has

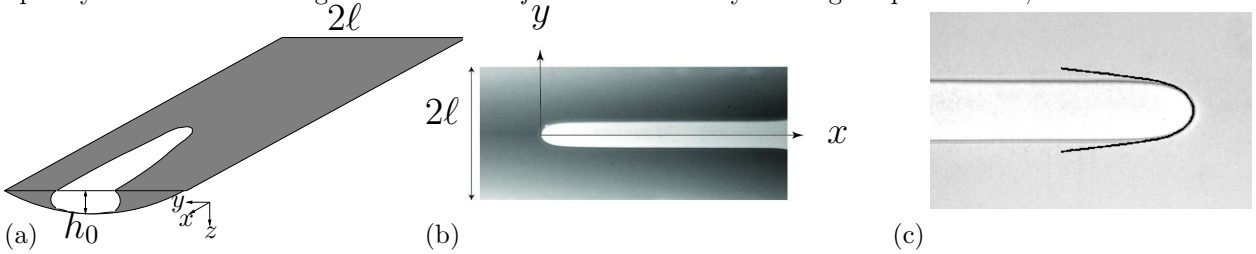

FIG. 1. (a) Perspective view of a sketch of an experimental mini-channel. The air bubble (in white) enters from one side of the mini-channel, while the liquid (in grey) is pumped out from the other side. (b) Top view of the experimental bubble shape in a mini-channel in the (x,y) plane which displays a shape denoted f(x). (c) Superimposition of the experimental finger shapes obtained in a longitudinally uniform channel on constricted one (in black), with a constant vertical to transverse aspect ratio $\epsilon = h_0/\ell$.

a constant curvature, the value of which has to be determined.

• Numerical analysis : we solved the free-boundary problem associated with a perfectly wetting liquid presenting an *a priori* unknown constant mean curvature κ :

$$-\frac{\partial_x^2 f}{(1+\partial_x f^2)^{\frac{3}{2}}} + \frac{2}{h(y)} = \frac{2}{h(f^\infty)} = \kappa \tag{1}$$

κ can be decomposed into an horizontal plane curvature which depends on $f(x)$ and the vertical plane principal curvature which is controlled by the local gap h. $f(x)$ presents an horizontal slope at $x \to \infty$, and a vertical one at $x = 0$. These conditions determine the value of κ. The *a priori* unknown asymptotic width f^∞—like the associated κ— is found with a shooting method out of a Runge–Kutta integration procedure. The result is depicted in figure 2.

• Asymptotic analysis : The channel under study presents a small parameter which is the gap to width ratio $\epsilon = h_0/\ell$. Using proper non-dimentionalization, one finds that problem (1) is singular.

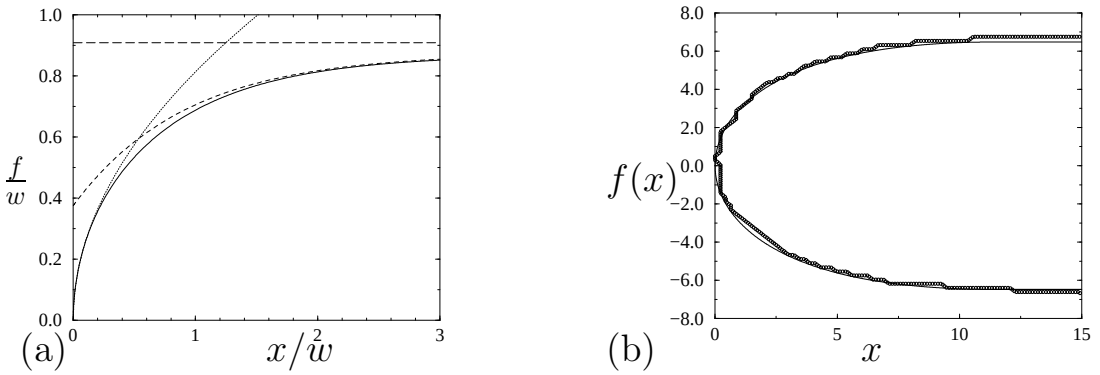

FIG. 2. (a) Numerical computation of in-plane interface shape $f(x)$ in continuous lines compared with asymptotic prediction with a channel aspect ratio $\epsilon = 10^{-2}$. Dotted lines represent the inner asymptotic behavior, dashed lines stand for the exponential decay of the outer solution. The results are non-dimentionalized by an intermediate length-scale which scales as $w = \epsilon^{1/3}\ell$ (b) Superimposition of the numerical computation and the experimental observations inside a quadratic shape $h(y)$ channel depicted in Figure 1a.

Moreover, the typical longitudinal length-scales f and x can be shown to vary with the gap to width ratio ϵ as the intermediate length-scale w defined as $w = \epsilon^{1/3}\ell$. This non-dimensionalization is successfully compared with numerical computation on figure 2a, where it is also observed that asymptotically matched inner and outer solutions satisfactorily compares with the numerical curve. This asymptotic analysis leads to a simple expression for the pressure drop needed to overcome capillary forces associated with surface tension γ :

$$\Delta P = 2\gamma(1 + (3/4)^{2/3}\epsilon^{4/3})/h_0. \tag{2}$$

This analysis can be directly extended to the case of a longitudinally varying channel. Figure 1c shows that the tip in-plane curvature is very close, for a longitudinally uniform channel or constricted channel having the same gap h_0. Similar conclusions can be drawn from extending previous asymptotic analysis[2].

III. INVASION PERCOLATION

The above analysis is extended to model the air invasion between complicated random surfaces. Experiments are similarly performed on specifically designed micro-channels obtained from numerically generated random surfaces (Fig. 3a). The network of the aperture saddle point is numerically computed (Fig. 3b), so that the invasion percolation rule (2) can be applied (Fig. 3c) using the local ϵ associated with each saddle point.

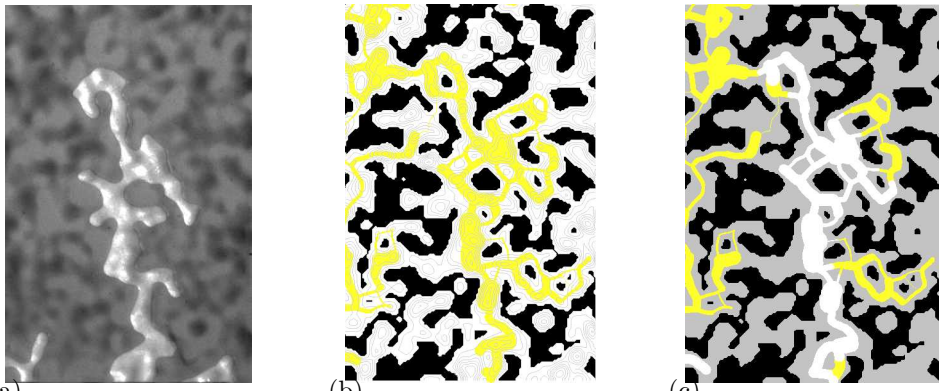

FIG. 3. (a) Drainage experiments between randomly generated surfaces, (b) Numerical extraction of the saddle point network, (c) Predicted invasion is represented in white.

[1] H. A. Stone and S. Kim, AichE Journal **47**, 1250 (2001).
[2] F. Plouraboué, S. Geoffroy, and M. Prat, forthcoming in Phys. Fluid, (2004).